4.2 GRAIN BOUNDARY STRENGTHENING PROPERTIES OF TUNGSTEN ALLOYS —

W. Setyawan and R. J. Kurtz (Pacific Northwest National Laboratory)

OBJECTIVE

The objective of this research is to support the search for tungsten alloys with increased grain boundary cohesion using first-principles methods.

SUMMARY

Density functional theory was employed to investigate grain boundary (GB) properties of W alloys. A range of substitutional solutes across the Periodic Table was investigated to understand the behavior of different electronic orbitals in changing the GB cleavage energy in the Σ27a[110]{525} GB. A number of transition metals were predicted to enhance the GB cohesion. This includes Ru, Re, Os, Ir, V, Cr, Mn, Fe, Co, Ti, Hf, Ta and Nb. While lanthanides, *s* and *p* elements were tended to cause GB embrittlement.

PROGRESS AND STATUS

Introduction

The development of novel W-based materials that are suitable for future fusion reactors is likely to involve synergistic advancements in intrinsic W alloys [1, 2], grain boundary (GB) engineering [3, 4] and W-based composites [5, 6]. In all of these areas, understanding and controlling the characteristics of materials at intergranular regions are important. Using first-principles methods, we have recently started to study the strengthening properties of substitutional solutes on the GB cohesion of tungsten. In our previous studies [7], the effects of the fifth- and sixth-row transition metals (TM) were investigated in three GB structures, Σ27a[110]{525}, Σ11[110]{323} and Σ3[110]{112}. GB strengthening was found for Hf, Ta, Nb, Ru, Re, Os and Ir for the Σ27a GB and to a lesser degree for the Σ11 GB. Lower valence solutes, with respect to W, strengthen the GB at certain substitutional sites, while higher valence elements enhance it at other positions. For the Σ3 GB, the Ru, Re, and Os slightly increased the cleavage energies. Hence, alloying with these TMs increases the cohesion more effectively for large-angle GBs whose cleavage energy, in general, is lower than the low-angle ones. Electron density plots elucidates the mechanism of charge addition or depletion of the GB bonding region upon alloying leading to stronger or weaker intergranular cohesion, respectively.

In this report, we extended the study to include a more complete list of solutes spanning the different characters of electronic valence across the Periodic Table. The fourth-row TMs (Sc to Zn), lanthanides, alkalis, alkaline earth metals, and *p*-electron solutes from Groups 3A-5A were investigated. Knowledge of how different types of valency and atomic volume differences affect the GB would provide a reference in designing tungsten-based materials with improved fracture resistance.

Formalism

In this study, the Σ27a[110]{525} tilt GB was used as a model. The GB structure was initially relaxed using conventional molecular dynamics (MD). We used the interatomic potential developed by Ackland and Thetford [8]. Systematic interfacial shifts and atoms relaxations were

done to achieve the most stable configurations. The structures obtained from the MD were further optimized via the ab initio method. VASP software was used to perform the quantum mechanical calculations based on the density functional theory (DFT). Accurate projector-augmented-wave pseudopotentials with Perdew-Burke-Ernzerhof exchange-correlation functionals were employed [9–11]. Plane-wave energy cutoffs and k-point sampling of the Brillouin zone were carefully checked for convergence. Spin-polarized calculations were performed. Structures were fully relaxed with a tolerance of 1 meV. For non-slab configurations, a force tolerance of 10 meV/A was used. At the end of volume-nonconserving relaxations, an additional static calculation was performed to avoid numerical errors due to basis incompleteness. The necessary slab thickness for the DFT calculations was determined from the convergence tests of the {525} surface energy. A total of 62 layers including one GB interface and two free surfaces were required for the Σ27a GB. A 1x2x1 supercell containing 124 atoms was used throughout the simulations.

RESULTS

Figure 1 shows the structure of the Σ27a GB as viewed from the <110> direction. An electron density plot reveals the alternating atomic layers along [110]. The unit cell contains four such layers. The slab thickness was carefully determined to include atoms with a "bulk-like" atomic environment (site O). The details of the convergence study of the slab thickness can be found in Ref [12]. The cube of the bcc with site O as the center is shown. The dashed lines represent the edges of the cube. Site O is eight-coordinated with nearest-neighbor (nn) distance of 2.73 Å. As the cube is viewed from [110] projection, only six nn atoms are visible. We introduce three types of coordination as follows:

nc: Site B is eight-coordinated with 8 nearest neighbors: A (2.73 Å), C (2.73 Å), F (2.79 Å) and H (2.66 Å), two atoms each. Even though the angular position of the neighbors deviates from the perfect bcc structure, the nn distances are similar to that of a single crystal. For this reason, site B is referred as "normally-coordinated" (*nc*).

oc: Site A represents an "over-coordinated" (*oc*) position with 10 nearest neighbors: G (2.46 Å), B (2.73 Å), E (2.56 Å), two atoms each and F (2.89 Å) four atoms.

uc: Site D is an "under-coordinated" (*uc*) position with 6 nearest neighbors: C (2.72 Å) two atoms and E (2.90 Å) four atoms.

The electron density plot (Fig. 1) reveals the bonding of atoms A, B and D with their visible neighbors. The charge distribution corroborates the coordination types of those sites. From this point of view, these three sites are good representatives to elucidate the important response of various orbital types to different atomic environments in the GB.

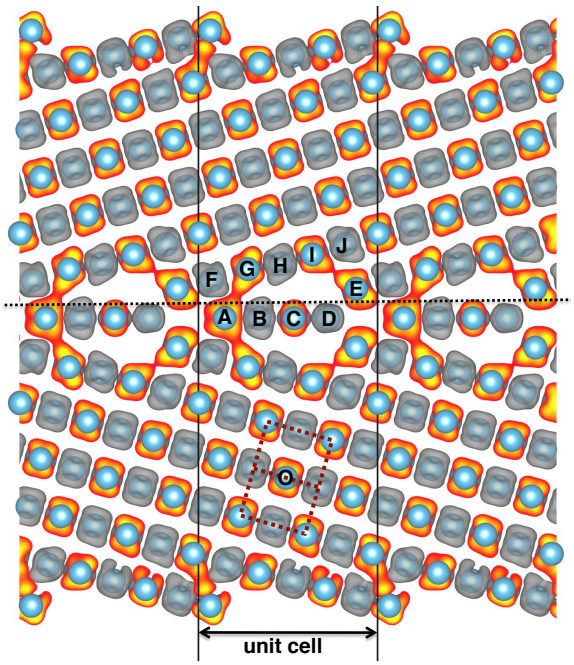

Figure 1. Structure and electron density of the W Σ27a[110]{525} tilt GB viewed along the <110> direction. The relative strength of the GB bonds is revealed (higher electron density indicates stronger bond).

Grain Boundary Strengthening

The GB strengthening property of a solute was studied by substituting one atom at sites A, B or D. This corresponds to ~ 2.6 at.% in bulk. The horizontal dashed line (Fig. 1) denotes the cleavage plane for calculating the cleavage energy (E_{cv}). Figure 2 shows the evolution of the cleavage energy as a function of atomic number of the solute at different substitutional positions. The line at 4.16 J/m^2 marks the cleavage energy of the pure GB. Systematic trends are evident and can be summarized as follows:

(i) *s*-valence: embrittlement at all sites, fewer electrons → lower E_{cv}. Substitution at *oc* site promotes lower cleavage energy.

(ii) *p*-valence: embrittlement at all sites, more electrons → lower E_{cv}. Substitution at *oc* site promotes lower cleavage energy.

(iii) *d*-valence: strengthening at *oc* site (maximum with 7B-8B elements) and *uc* site (maximum with 3B-4B solutes), but embrittlement at *nc* site.

(iv) *f*-valence: embrittlement at all sites except Lu and Tm at *uc* site, fewer electrons → lower E_{cv}. Substitution at *oc* site promotes lower cleavage energy. Note that La and Lu may also be assigned to the *d*-valence group since their *f*-orbitals are well screened.

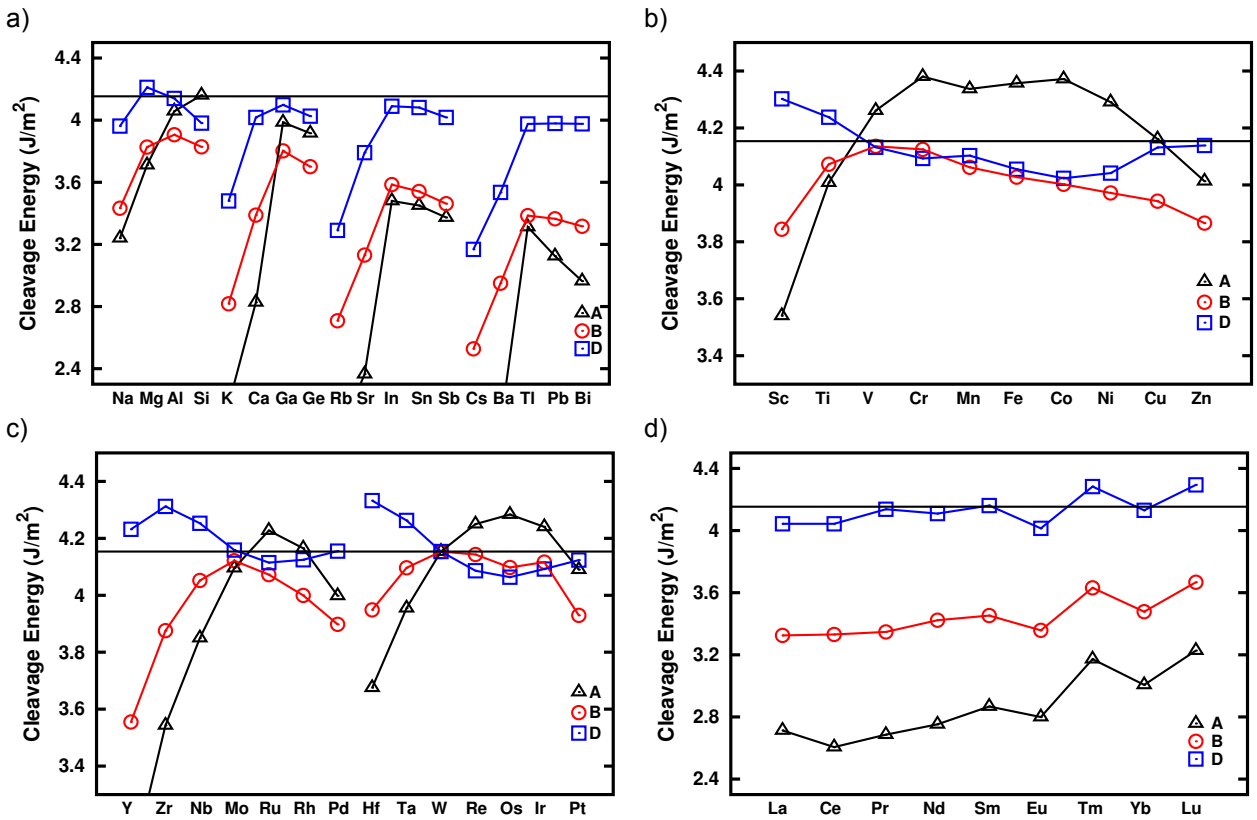

Figure 2. Cleavage energy of W Σ27a GB as a function of solutes substituted at positions A, B and D in Fig. 1. The elements are arranged with increasing atomic number. a) *sp*-valence elements, b) transition metals row-4, c) transition metals row-5 and row-6, and d) lanthanides. The line at 4.16 J/m^2 marks the cleavage energy of the pure GB.

These results indicate that strengthening can be achieved by using solutes near the middle region of the Periodic Table. Towards the edges of the Periodic Table, embrittlement is enhanced. The behavior of lanthanides is in between that of Ba and Hf.

Among the strengthening solutes, those with a smaller valency than W strengthen at *uc* site. The mechanism is that these solutes give off some electrons to the nearby *oc* site governing the most GB bonding, hence increasing the cohesion. On the other hand, higher-valence metals increase the cohesion at *oc* site by providing more electrons to be available for bonding. The bonding is mediated by the *d*-orbitals. At the *oc* site, the maximum strengthening is produced by Os, Ru, and near Fe, which is due to the fact that these atoms, with six electrons, complement tungsten's four electrons to fully occupy the *d*-orbitals. At the *nc site,* all solutes decrease the cleavage energy. This is caused by the redistribution of the electrons between the solute at this site and W at the *oc* site, which results in a net decrease of in GB bonding. A list of the potential strengthening solutes is presented in Table 1 along with their maximum solubility at several temperatures.

Table 1. Solubility limit [atomic %] of potential alloying elements in W at several temperatures T. Solutes that increase the grain boundary cohesion when substituted at over- or under-coordinated site are grouped in the top or bottom panel, respectively [13, 14]. Several data are not available (N/A).

T [°C]	V	Cr	Mn	Fe	Co	Ni	Ru	Re	Os	Ir
0	100	<4.8	N/A	2.1	7.2	1.2	6.3	19.7	5	<1.7
500	100	4.8	N/A	2.1	7.2	4.8	6.3	22.6	5	<1.7
1000	100	11.2	N/A	2.4	7.3	6.2	6.3	25.7	5.7	1.7
1500	100	26.5	N/A	2.7	8.8	4.6	8.2	27.8	6.9	2.4
	Mg	Sc	Ti	Y	Zr	Nb	Hf	Ta	Lu	
0	N/A	~0	<11.1	N/A	0.7	100	<3.4	100	~0	
500	N/A	~0	11.1	N/A	0.7	100	<3.4	100	~0	
1000	N/A	~0	44	N/A	0.8	100	3.4	100	~0	
1500	N/A	~0	100	N/A	1.3	100	6.2	100	~0	

Substitutional Solute Stability

Figure 3 shows the segregation energy of a substitutional solute relative to the configuration when the solute is at the “bulk-like” site O in the same simulation cell. A negative value of segregation energy indicates that the solute is more stable at the GB site than in the bulk. For any solute, the most stable configuration results in the highest cohesion. The most important finding is that solutes that potentially increase the cleavage energy are stable at their corresponding GB site. Therefore, energetically, their strengthening properties as predicted in this study can be realized.

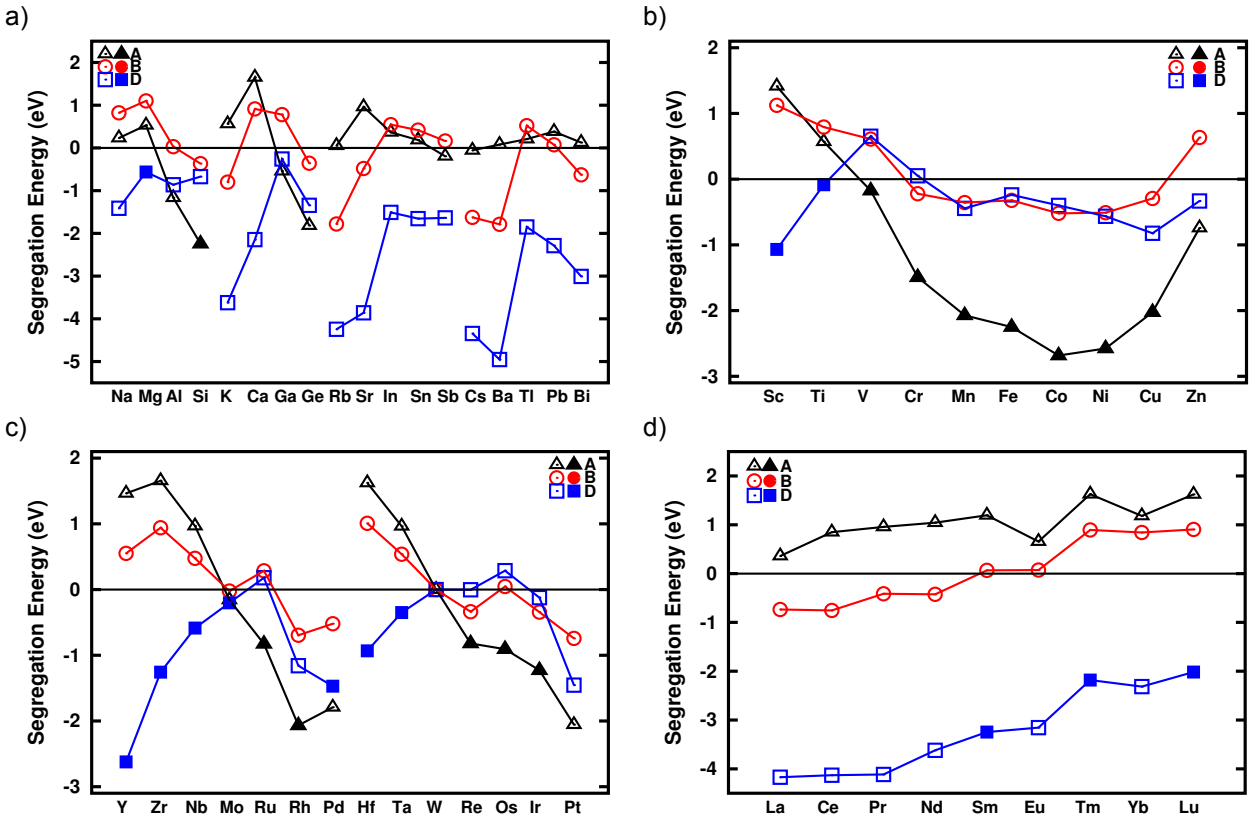

Figure 3. Segregation energy of substitutional solutes in W Σ27a GB relative to "bulk-like" site in the same simulation cell. The more negative the segregation energy the more stable it is at that site. The combinations of atom and position that increase or decrease the GB cohesion are plotted in filled or open marks, respectively.

Computations were performed partly on Chinook supercomputer (EMSL-45390) at Pacific Northwest National Laboratory (sponsored by the DOE's Office of Biological and Environmental Research).

REFERENCES

[1] Y. Mutoh, et al., *J. Mater. Sci.* **30** (1995) 770.
[2] S. Wurster, et al., *J. Nuc. Mater.* **413** (2011) 166.
[3] L. J. Kecskes, et al., *Mater. Sci. Eng. A* **467** (2007) 33.
[4] M. Faleschini, et al., *J. Nucl. Mater.* **367** (2007) 800.
[5] E. Lassner and W. -D. Schubert, "Tungsten", Springer (1995).
[6] Y. Ishiyama, et al., *Mater. Sci. Eng. A* **473** (2008) 7.
[7] W. Setyawan and R. J. Kurtz, Semiannual Report period ending December (2011).
[8] G. J. Ackland and R. Thetford, *Phil. Mag. A* **56** (1987) 15.
[9] P. E. Blöchl, *Phys. Rev. B* **50** (1994) 17953.
[10] G. Kresse and D. Joubert, *Phys. Rev. B* **59** (1999) 1758.
[11] J. P. Perdew, K. Burke and M. Ernzerhof, *Phys. Rev. Lett.* **77** (1996) 3865.
[12] W. Setyawan and R. J. Kurtz, *Scrip. Mat.* **66** (2012) 558.

[13] Alloy Phase Diagram, in ASM Handbook Online Vol. III (2012).
[14] T. B. Massalski, et al., Binary Alloy Phase Diagram, ASM International, Metals Park (1986).